ACS APPLIED MATERIALS & INTERFACES

Research Article

www.acsami.org

Trafficking of Gold Nanorods in Breast Cancer Cells: Uptake, Lysosome Maturation, and Elimination

Weiqi Zhang,[†] Yinglu Ji,[‡] Xiaochun Wu,*[,‡] and Haiyan Xu*[,†]

[†]Institute of Basic Medical Sciences, Chinese Academy of Medical Sciences and Peking Union Medical College, Beijing 100005, P. R. China

[‡]CAS Key Laboratory of Standardization and Measurement for Nanotechnology, National Center for Nanoscience and Technology, Beijing 100190, P. R. China

Supporting Information

ABSTRACT: Gold nanorods (AuNRs) have been largely investigated driven by their promising potentials in drug delivery, imaging, and photodynamic therapy because of their distinctive physicochemical properties. It is widely known that AuNRs can be taken up by different cells, however, the trafficking of the nanorods in cells are less known. In this work, the behaviors and fate of AuNRs in the human breast cancer cell line MDA-MB-231 were intensively probed by transmission electron microscopy (TEM) with detailed time resolution, together with induced couple plasmon mass spectroscopy (ICP-MS), confocal microscopy, Western blot, and cell viability assay. We reveal that AuNRs enter the classic lysosome maturation through endocytosis and are sequestered in the vesicular system even during cell division. AuNRs can escape from the lysosomes occasionally and the escaped AuNRs are recycled back into the lysosomal system through cytoprotective autophagy. The dilution of AuNRs in cells is mainly attributed to the cell division rather than exocytosis, because expelled AuNRs can be re-endocytosed by the cells. The feature of vesicular restriction guarantees other organelles such as mitochondria and nucleus are exempted from the direct exposure to AuNRs.

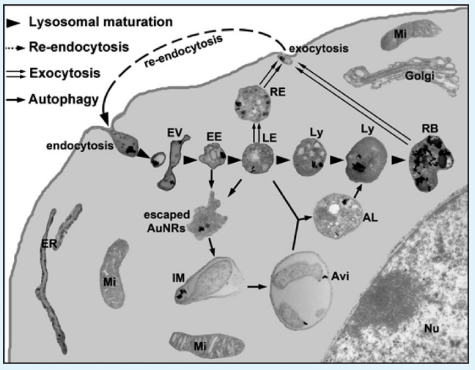

KEYWORDS: *autophagy, cellular trafficking, gold nanorods, toxicology, transmission electron microscopy*

INTRODUCTION

Gold nanorods (AuNRs) have been widely explored in drug delivery, photothermal therapy, biosensing, and imaging because of their attractive optical properties.[1−3] When AuNRs act as drug delivery vehicle, imaging contrast, or thermotherapeutic reagent, they are reported to be taken up by the cells and mainly locate in lysosomes.[4−6] The eventual functionalities of AuNRs in above applications are largely dependent on their trafficking behaviors as well as their location in cells. For example, siRNA can only induce effective gene silencing when located in cytoplasm, and therefore efficient lysosomal escape is expected in siRNA delivery mediated by AuNRs.[7,8] When used as imaging modules to track cells, restriction of AuNRs in vesicles and minimizing the exocytosis process are more relevant for magnifying signals and increasing the tracking time.[9] Although it is widely known that AuNRs can be taken up by different cells, and the uptake as well as the cytotoxicological studies of AuNRs have achieved much progress in the past decade,[10−12] the trafficking of AuNRs in cell such as how they reach the lysosome, what their long-term fate is, etc., has been less known to date.

Dark-field, two-photon fluorescent and fluorescent confocal microscopes are important tools for studying cellular uptake of AuNRs in the living cells.[13−15] But these visualizing methods have limited resolution in identifying AuNRs in the cellular ultrastructures, especially when the intracellular AuNRs are rare. Furthermore, to colocalize AuNRs with organelles, immunofluorescence or organelle-specific dyes staining are commonly needed, which brings out unavoidable false-positive or false-negative results. Compared with above light microscopes, transmission electron microscopy (TEM) provides an alternative powerful tool to distinguish single AuNRs in the cells. First, AuNRs have high electron density and their shape is distinctive from the cellular components. Second, ultrastructural characteristics of cellular organelles have been well documented in the past few decades by physiologists.[16−19] The two facts allow us to identify the AuNRs' ultrastructural location clearly and easily.

Under above backgrounds, we synthesized AuNRs coated with cationic polyelectrolytes and probed their trafficking in a breast cancer cell line MDA-MB-231 by intensive TEM observation at different incubation and chasing time points in combination with analysis of induced couple plasmon mass spectroscopy (ICP-MS), confocal microscopy and Western blot. We found that AuNRs were sequestered in the lysosomal system even during cell mitosis, while those occasionally

Received: August 13, 2013
Accepted: September 13, 2013
Published: September 13, 2013

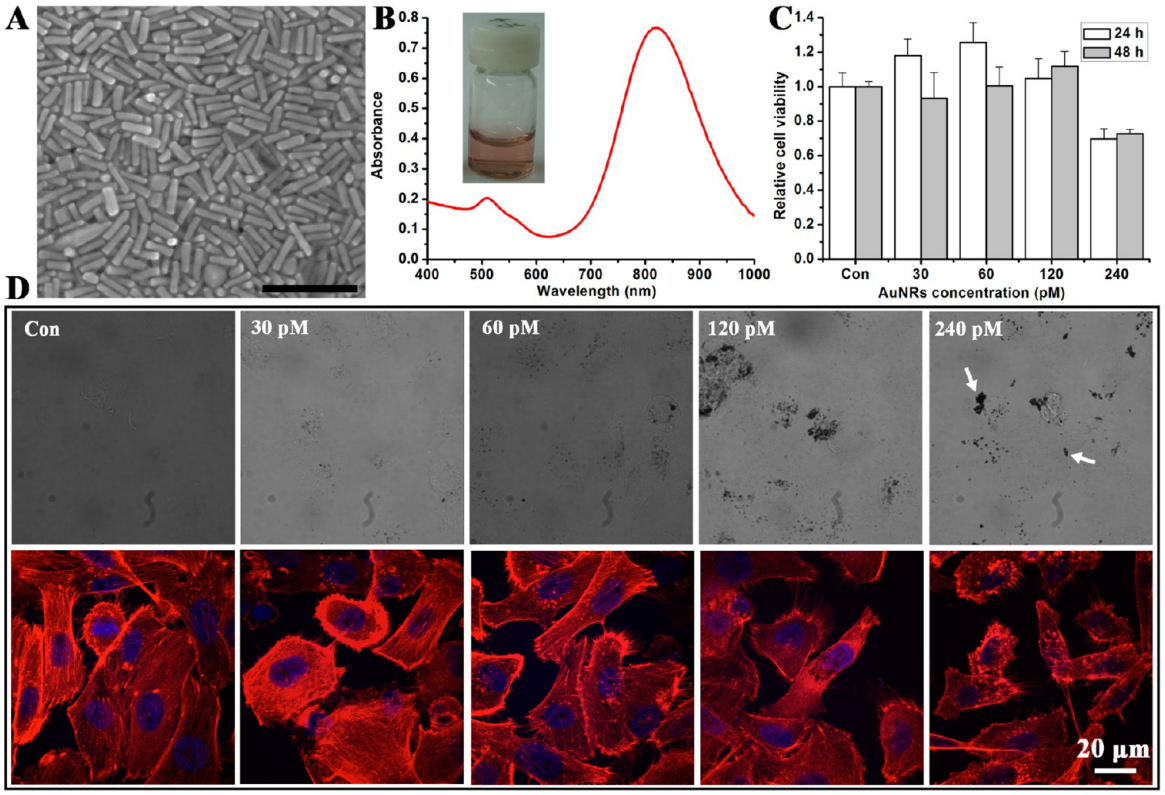

Figure 1. Characterization and cytotoxicity evaluation of AuNRs. (A) SEM images of as-synthesized AuNRs. The scale bar represents 200 nm. (B) UV−vis−NIR absorption curve of AuNRs aqueous solution. The inserted image is the corresponding photograph. (C) CCK-8 assay of MDA-MB-231 cells after 24 or 48 h incubation with AuNRs at different concentrations. (D) Actin staining of MDA-MB-231 cells after 48 h incubation with AuNRs. The nucleus is stained blue by DAPI and actin filament is stained red with rhodamine-labeled phalloidine. The white arrow points the aggregates of AuNRs out of the cells.

escaped into the cytoplasm could be recycled back into lysosomes by autophagy. The dilution of AuNRs in the cells was mainly attributed to the cell division rather than exocytosis, because expelled AuNRs were re-endocytosed by the cells.

MATERIALS AND METHODS

Reagents and Materials. Silver nitrate ($AgNO_3$), cetyltrimethylammonium bromide (CTAB), hydrogen tetrachloroaurate (III) trihydrate ($HAuCl_4{\cdot}3H_2O$), L-ascorbic acid and sodium borohydride ($NaBH_4$) were obtained from Alfa Aesar. Poly sodium-p-styrenesulfate (PSS, molecular weight: 70000) and poly diallyldimethyl ammonium-chloride (PDDAC, 20%), glutaraldehyde, tween-20 and tetramethylrhodamine-conjugated phalloidin were purchased from Sigma-Aldrich. Bovine serum albumin was purchased from MP biomedicals. Leibovitz's L-15 (L15) culture medium and fetal bovine serum were purchased from Gibco.

Preparation and Characterization of AuNRs. The synthesis of PDDAC-coated AuNRs was described in our previous work.[20] The concentration of AuNRs was expressed as number of nanorods instead of gold atoms. To observe the morphology of AuNRs, 10 μL AuNRs solution was dropped on a silicon wafer and left dried. The scanning electron microscopic (SEM) observation of AuNRs was performed on a Hitachi S-5200 scanning electron microscope. The absorption spectrum of AuNRs in the range of 400−999 nm was recorded on a Perkin-Elmer UV−vis/near-infrared spectrophotometer (Lamdba 950).

Cell Culture. MDA-MB-231 cells were obtained from the Cell Resource Center of Chinese Academy of Medical Sciences (Beijing, China). The cells were cultured in L15 medium with 10% serum, 100 U/ml penicillin, 100 U/ml streptomycin and maintained at 37 °C in a humidified incubator with a low-CO_2 environment as L15 medium can support cell growth in environments without CO_2 equilibration.

Cellular Viability Assay. The viability of cells after the incubation with AuNRs was evaluated using the Cell Counting Kit-8 (CCK-8) (Dojindo Molecular Technologies, Inc.). Briefly, about 8000 cells per well were plated on 96-well plates. After an overnight incubation, 100 μL media containing various concentrations of AuNRs were added into the plates. The cells were incubated with AuNRs for 24 or 48 h, then the cells were rinsed twice with PBS and 110 μL fresh medium with 10 μL CCK-8 solution was added. After an incubation of 2 h in 37 °C, 100 μL of supernatant was subjected to the absorption measurement (BioTek Synergy 4 Hybrid Multi-Mode Microplate Reader) at the wavelengths of 450 and 630 nm. The absorbance at 630 nm was set as background and the viability of the control cells was set as 100%.

Actin Staining. About 4×10^4 cells/well were seeded on coverslips in 24-well plates and cultured overnight to allow cell adhesion. After incubation with 0.5 mL media containing various concentrations of AuNRs for 48 h, the cells were fixed with 1% paraformaldehyde for 15 min. The cells were washed thrice with PBS and incubated with permeabilization buffer (0.5% Triton X-100/PBS) at 4 °C for 5 min. Then the cells were rinsed thrice with PBS and incubated with 1% PBS/BSA at 37 °C for 5 min. After that, cells were stained by tetramethylrhodamine-conjugated phalloidin (1: 500 dilution) for 40 min. Then the cells were washed thrice with 0.5% tween-20/PBS. Finally, the coverslips were mounted using an aqueous mounting medium containing DAPI (Zhongshan Goldenbridge biotechnology Co, Beijing, China). The cells were visualized with an UltraVIEW VoX laser confocal microscope (Perkin-Elmer).

Transmission Electron Microscopic Observation. About 1×10^6 cells were seeded in 100-mm Petri dish and left overnight to allow cell adhesion. Cells were incubated with 10 mL medium containing 60 pM AuNRs for 0.25, 0.5, 0.75, 1.5, 3, 6, 12, 24, and 48 h. The cells were rinsed thrice with cold PBS and scraped gently from the dish. The cells were collected and fixed with 2.5% glutaraldehyde in cold

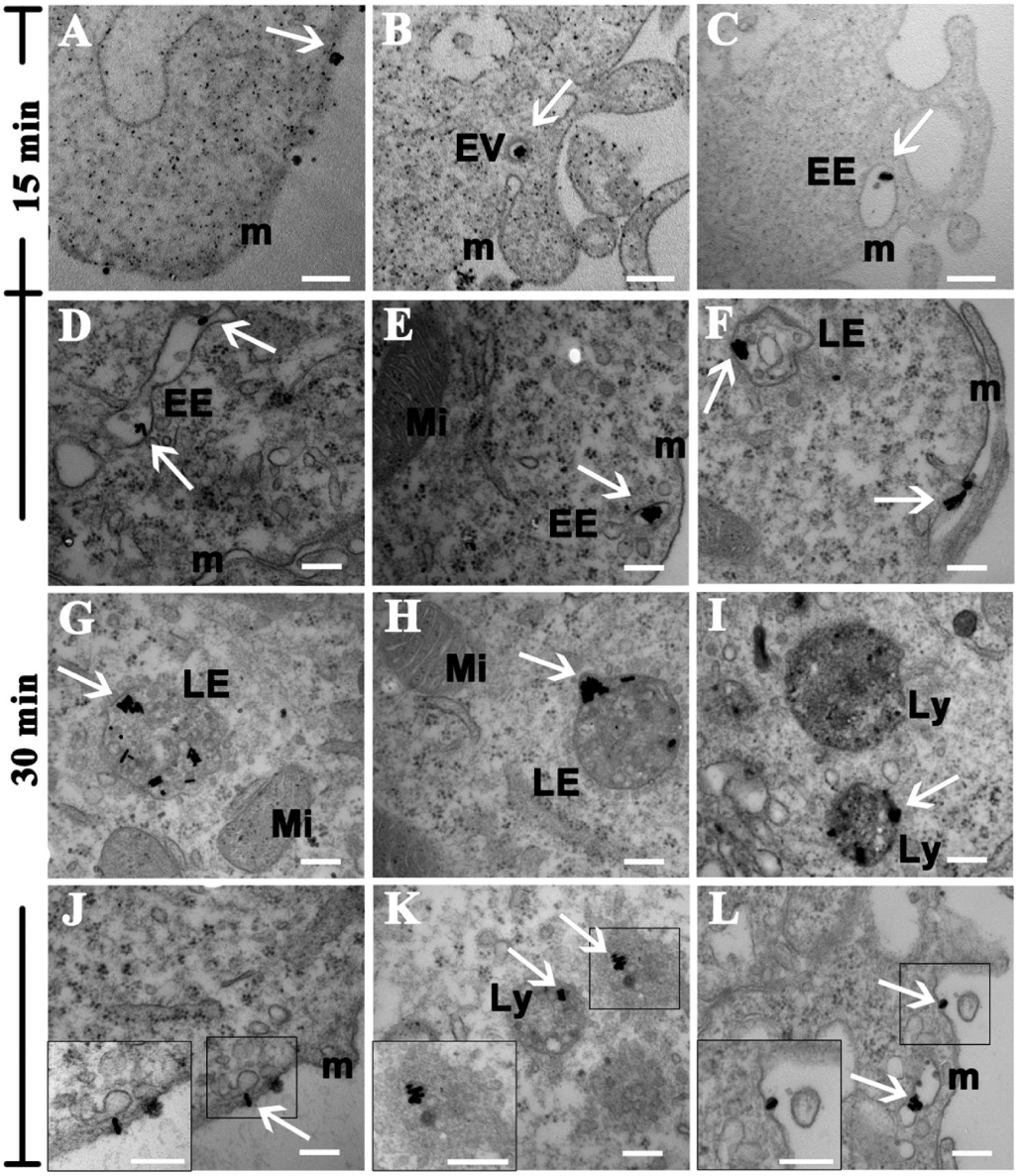

Figure 2. Representative images of AuNR-containing ultrastructures after (A–C) 15 and (D–L) 30 min incubation with AuNRs. (A) AuNRs adsorbed on cellular membrane. (B) Receptor-mediated endocytosis of AuNRs. (C–E) Early endosome (EE). (F–H) Late endosome (LE). (I) lysosome (Ly). (J) AuNRs on vertically penetrating cell membranes. (K) A few of AuNRs are free in the cytoplasm, whereas others are sequestered in intact lysosome of the same cell. (L) AuNRs associated with electron dense substances are located around the cells. The white arrow points the location of AuNRs and the scale bar represents 200 nm. EV, endocytic vesicle; Mi, mitochondrion; m, cellular membrane.

phosphate buffer (PB) for at least 1 h. Then the cell pellets were further postfixed in 1% osmium tetroxide in PB. After gradual dehydration with alcohol, the cells were embedded in Epon. Ultrathin sections were cut and stained by uranyl acetate. The ultrastructural observation was performed on a JEM-1010 transmission electron microscope with different magnifications.

To probe the exocytosis of AuNRs, the cells were pulsed with 60 pM AuNRs for 30 min. The cells were washed thrice with PBS and incubated in fresh culture medium for another 0.25, 0.5, 1, 2, and 6 h. Then the cells were harvested for TEM sample preparation.

To probe the AuNRs' behavior in cell division, cells in 3 dishes were incubated with AuNRs for 24 h. Then the medium was replaced with fresh culture medium without AuNRs. After 24 h incubation, cells were passaged. The subcultivated cells were further successively passaged for 6 times every 2 days. During the passaging process, the subcultivation ratio was fixed at 1:3 and parts of cells were collected for TEM and ICP-MS analysis.

ICP-MS Analysis. To measure the amount of AuNRs expelled by cells, we seeded 1.6×10^5 cells in 6-wells plate. After the incubation with 60 pM AuNRs in 2 mL of medium for 30 min, the wells were washed thrice with PBS. The medium was replaced with 2 mL of fresh medium without AuNRs. After 0.25, 0.5, 1, 2, and 6 h of incubation, the incubated medium (2 mL) was collected, meanwhile the wells were washed twice with 1 mL of PBS. The incubated medium and washing PBS were combined together and designated as supernatants (4 mL). To eliminate the dead cells, the supernatants were filtered through a 5 μm nylon membrane filter. Then 1 mL of the filtered supernatant was subjected to the ICP-MS sample preparation. The experiments were conducted in triplicate. The mass of gold determined from the ICP-MS was converted to the number of AuNRs using the calculated number of gold atoms per nanorods.[12]

ICP-MS Sample Preparation. One milliliter of supernatant or 1.5×10^5 passaged cells were mixed with 10 mL of aqua water containing 10% H_2O_2 and subjected to the microwave digestion (Mars 5, CEM, USA). Then the solutions were diluted to 40 mL and the Au elements

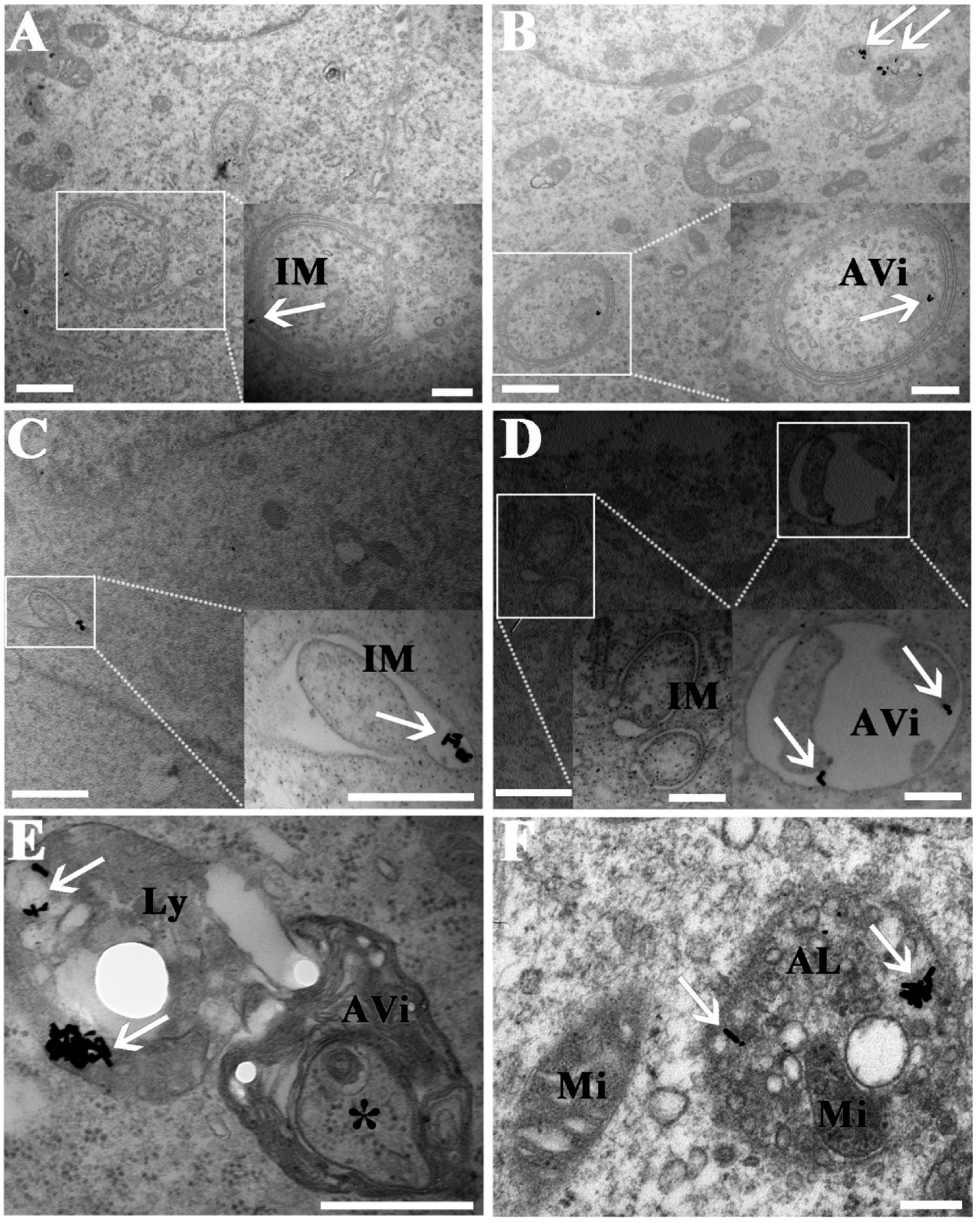

Figure 3. AuNRs enter the autophagosome of the cells. (A, C) Representative images of AuNRs located in isolation membrane (IM). (B, D) AuNRs are sequestered in immature autophagosome (AVi). The rectangular region is further magnified at the bottom and the scale bar in the image and magnified image represents 1 μm and 200 nm, respectively. (E) AuNR-containing lysosome on fusing with AVi. The asterisk labels the cytoplasmic component in AVi. (F) AuNRs located in autolysosome (AL) with mitochondria (Mi) enclosed in. The scale bar represents 200 nm.

were measured on a Thermo ICP-MS XII instrument (Thermo-Fisher).

Western Blot. 1.6×10^5 cells were plated in 6-well plates and incubated overnight to allow cell attachment. The cells were incubated with 60 pM AuNRs in 2 mL medium for 24 or 48 h, and then lysed on ice using RIPA (Beyotime, Jiangsu, China). Total proteins were harvested and denatured with SDS sample buffer. Then the proteins were separated with SDS-PAGE and blotted to polyvinylidene difluoride membranes (Millipore). The membrane was probed with anti-Beclin-1, anti-LC-3 and antiactin antibodies (Cell Signaling Technology). Appropriate HRP-conjugated secondary antibodies (Jackson Immunoresearch) and enhanced ECL chemiluminescence reagents (Millipore) were used to visualize the bands. The optical density (OD) of the bands was determined using Quantity One software (Biorad).

Statistic Analysis. Quantitative data are expressed as mean ± SD. Statistical analysis was performed using the 2-sided Student's t test. $p < 0.05$(*) and $p < 0.01$(**) represent statistically significant difference.

RESULTS AND DISCUSSION

Characterization and Cytotoxicity Evaluation of AuNRs. The positively charged AuNRs were prepared using seed-mediated method and the further modification with PSS (poly sodium-p-styrenesulfate) and PDDAC (poly diallyldimethyl ammoniumchloride) via layer-by-layer assembly.[20] As shown in Figure 1A-B, the dimension of AuNRs is about 13.5 × 57 nm and the two localized surface plasmon resonance peaks are located around 511 and 812 nm, respectively. Prior to the cell trafficking investigation, CCK-8 assay and actin staining were employed to determine a proper concentration of AuNRs that did not affect cells viability and cytoskeletal structure which plays vital roles in cellular endocytosis, transportation and cell division.[21] The results indicated exposure to 30−120 pM of AuNRs for 2 days was safe for the MDA-MB-231 cells, since most of the cells remained their viability (Figure 1C). As shown

dx.doi.org/10.1021/am4033857 | ACS Appl. Mater. Interfaces 2013, 5, 9856−9865

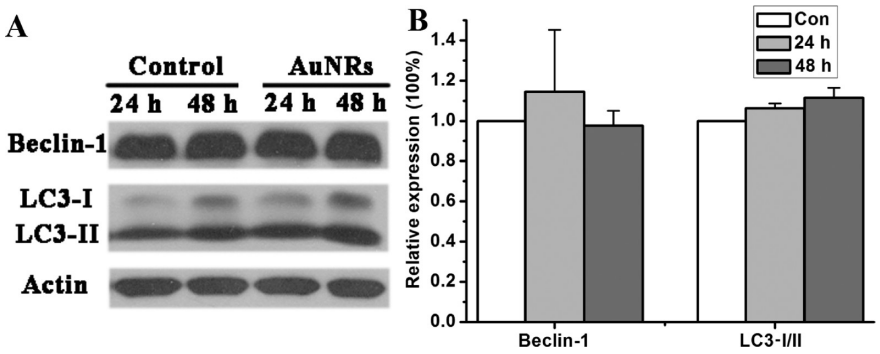

Figure 4. AuNRs have minimal effects on autophagy induction at safe dosage. (A)Western blot of the Beclin-1, LC3 proteins in MDA-MB-231 cells after 24 and 48 h incubation. The actin is set as the inner control. (B) Expression of Beclin-1 and LC3-I/II relative to that of actin.

in Figure 1D, actin filament structure of the cells is almost intact after the treatment with 30 pM or 60 pM of AuNRs, whereas part of the actin filament is depolymerized upon AuNRs exposure at 120 and 240 pM, and morphology of the cells exposed to AuNRs of 240 pM is even shrink dramatically. It has been reported that PDDAC-coated AuNRs induced ROS generation,[12] consequently high dosage of AuNRs may result in accumulated intracellular ROS, which could induce a cytoskeletal depolymerization.[22] In addition, aggregates of AuNRs were also observed out of the cells when the concentration reached 240 pM (white arrows in Figure 1D), suggesting a poor dispersibility of AuNRs in culture medium at this concentration. Taking above factors into account, 60 pM was chosen as safe AuNRs concentration in subsequent experiments to guarantee the cellular functions such as endocytosis and transportation were not significantly affected. This concentration of AuNRs was previously used to effectively deliver siRNA to silence protease-activated receptor-1 (PAR-1) gene.[6]

AuNRs Enter the Lysosome Maturation. In classic lysosome maturation, early endosomes (EE), late endosomes (LE), lysosomes (Ly), and residual body (RB) appear in a spatial and temporal order.[16−18,23] We hypothesized that AuNRs reached the lysosomes following the lysosome maturation after their internalization. To verify this point, distribution of AuNRs in the cells was examined from only 15 min up to 48 h of exposure since the endocytosis could be completed in 15 min.[24] As shown in Figure 2A−C, AuNRs are adsorbed on the cellular membrane and only appear in the endocytotic vesicle (EV) after 15 min of incubation. And one AuNR-containing vesicle featured with electron-dense outer layer was observed (Figure 2B). The electron-dense coat was considered derived from the clathrin assembling round the vesicle,[16,25] strongly suggesting the internalization of AuNRs was dependent on receptor mediated endocytosis (RME). After the clathrin coating was disassembled, the vesicle presented as endosomal structure (Figure 2C).[25] The RME of AuNRs was also evidenced by Wang et al. based on the experiments with endocytic inhibitors.[26] With incubation time elongated to 30 min, AuNRs were transported to various vesicular structures including EE, LE and lysosomes (Figure 2D−I), all of which are natural structures appearing in classic lysosome maturation.[27] It is noted that AuNRs gradually aggregated in the lysosomal structures, possibly because of the low pH environment and varied ionic strength in the lysosomes.[25,28] After 45 min incubation, AuNR-containing lysosomes appeared as polymorphic (see the Supporting Information, Figure S1). The fusion process (see the Supporting Information, Figure S1B) made AuNRs concentrate in the vesicles and increased the aggregation size of AuNRs. Six hours later, AuNRs began to appear in residual body (RB) which is inhomogeneous with electron dense structure (see the Supporting Information, Figure S1E), indicating that AuNRs reached the end point in lysosome maturation. Because AuNRs are highly inert and cannot be digested by the lysosomes, it was reasonable that AuNRs stayed with electron dense substances in RB. In addition to adsorbing on the cell membrane at the sidewall of AuNRs, single AuNR vertically penetrating the cellular membrane was observed in some occasions (Figure 2J). This suggests tip-entry may exist in the AuNRs uptake process as modeled by dynamic simulations,[29,30] nevertheless, percentage of this uptake pattern still calls for more researches.

It was interesting that AuNRs escaping from lysosomes were observed occasionally (Figure 2K); however, no accumulation of AuNRs occurred in the cytoplasm and most of the AuNRs were restricted in the vesicular system. Another notable phenomenon was that electron dense substances were adhered on the AuNRs appearing around the cell membrane after 30 min incubation (Figure 2L), whereas the AuNRs surface was clear when appearing near the cell membrane after 15 min of incubation. These phenomena suggested that (1) the escaped AuNRs were eliminated from cytoplasm by the cells using certain mechanism; (2) the "dirty" AuNRs near the cell membrane may be exocytosed by the cells, because it is unlikely that the components in the culture medium have such a high electron density. Motivated by figuring out what other processes happened along with AuNRs entering lysosome maturation, we next investigated cellular ultrastructures with a focus on autophagy and exocytosis.

AuNRs Escaping from Lysosomes Are Recycled by Cytoprotective Autophagy. As mentioned above, occasionally lysosomal escape of AuNRs was observed, which may result from the aging and rupture of lysosomes. Meanwhile, AuNRs were also observed in autophagosomes presenting as double or multiple membrane vesicles with cellular contents enclosed in Figure 3. As shown in panels A and C in Figure 3, AuNRs in the cytoplasm are surrounded by isolation membrane (IM) which is formed by flattering and curvature of an endosome-like structure.[31] With the expansion and closure of IM, AuNRs in the cytoplasm were sequestered in the autophagosomes (Figure 3B, D). After that, autophagosome fused with lysosomes and matured into autolysosomes (Figure 3E, F). One key function of autophagy is eliminating the unneeded materials in cells such as aged organelles and intracellular pathogens.[32] If pathogens

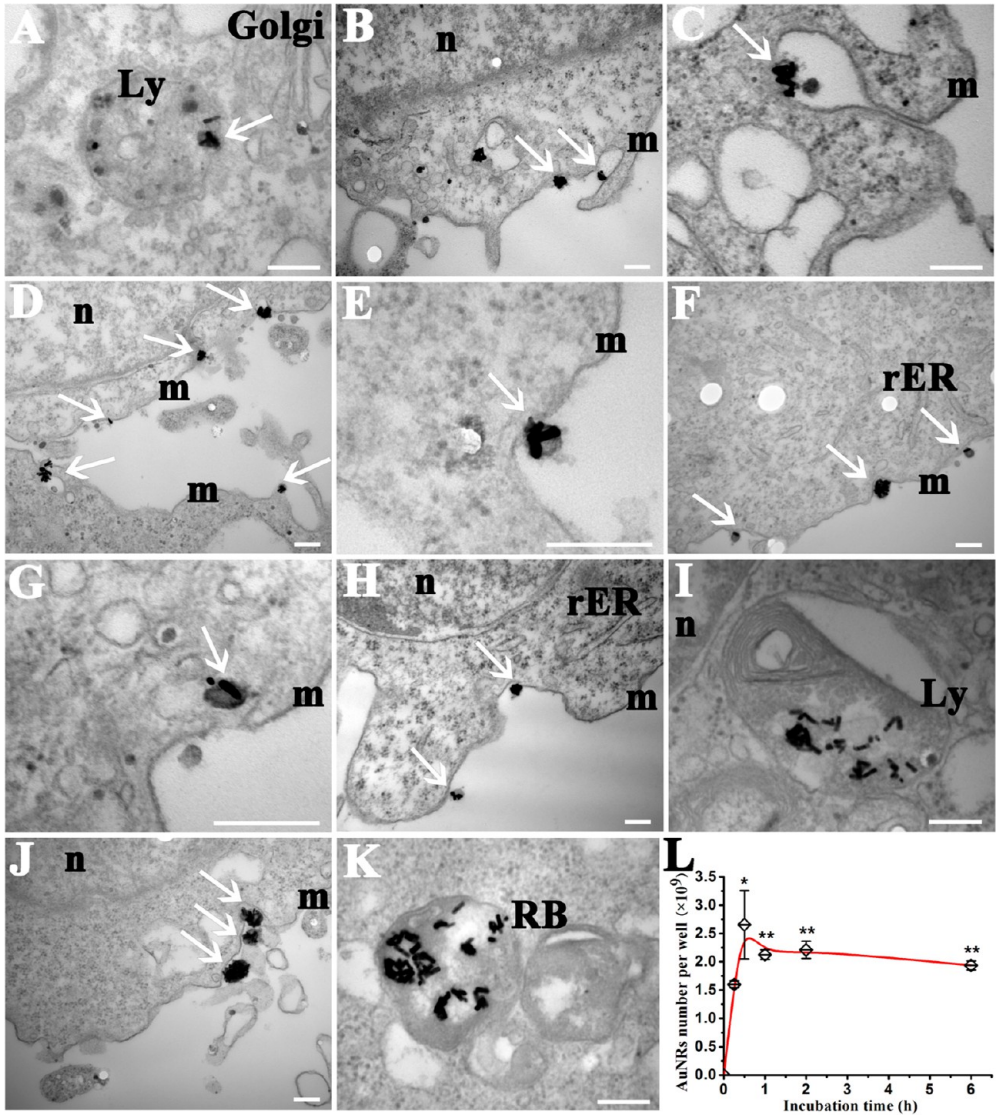

Figure 5. Exocytosis of AuNRs. After 30 min pulse of AuNRs, AuNRs in the cells were further chased for 0.25 (A–C), 0.5 (D, E), 1 (F–J), 2 (H–I) and 6 h (J–K). (A) AuNRs are associated with electron dense substances in the lysosome. (C, E, G) AuNRs along with electron dense substances are being exocytosed by the cell. (I) AuNRs are observed in lysosome containing multilayer membranes. (K) AuNRs appear in residual body. The white arrows point the AuNRs together with electron dense substances and the scale bar represents 200 nm. Golgi, golgi apparatus; rER, rough endoplasmic reticulum; RB, residual body; n, nucleus; m, cellular membrane. (L) The amount of Au in the supernatant measured by ICP-MS within the chasing time. The exocytosed AuNRs is expressed as number of AuNRs per culture well. '*'and '**' represent statistically significant difference from that of 0.25 h chasing.

(e.g., *Streptococcus*) escape from the vesicular system, they will induce autophagy and ultimately the pathogens are sequestered in lysosomal system again.[33] Therefore, the observed autophagy was considered responsible for recycling the AuNRs escaping from the vesicular system. When the cells detected AuNRs presenting in the cytoplasm, they tried to degrade the AuNRs by autophagy, otherwise AuNRs would accumulate in cytoplasm with incubation time elongated.

As autophagy is constitutively existed in cells to maintain the homeostasis of the cells,[34] Western blot of Beclin 1 and LC3 was conducted to probe whether AuNRs at 60 pM changed the autophagy level in cells. Beclin 1 is associated with the early autophagy and most of the Beclin 1 proteins are observed on isolation membranes rater than complete autophagosomes.[35] LC3-I is unlipidated LC3 and located in cytoplasm, whereas LC3-II is the lipidated form of LC-3 and localized on autophagosomal membranes. The conversion of LC3-I to LC3-II is associated with the autophagosome formation.[35] Results showed that the expression of Beclin-1 and LC3-I/II of the cells treated with AuNRs were very similar to those of the control (Figure 4). Meanwhile, no obvious accumulation of autophagic vacuoles in cells was observed in comparison to the control (see the Supporting Information, Figure S2), indicating that AuNRs at current dosage did not alter the autophagy level of the cells. The low autophagy level can partly explain the insignificant cytotoxicity of AuNRs under this concentration as elevated level of autophagy results in cell death.[36−39] Collectively, we consider that autophagy plays a cytoprotective role when cells are encountered with AuNRs in cytoplasm, which assures AuNRs are sequestered in the lysosomal systems for "degradation".

AuNRs Are Exocytosed and Re-endocytosed. The lysosomal system is dynamic and the cargos in this system are expected to recycle back to the cell surface, namely cell

dx.doi.org/10.1021/am4033857 | ACS Appl. Mater. Interfaces 2013, 5, 9856−9865

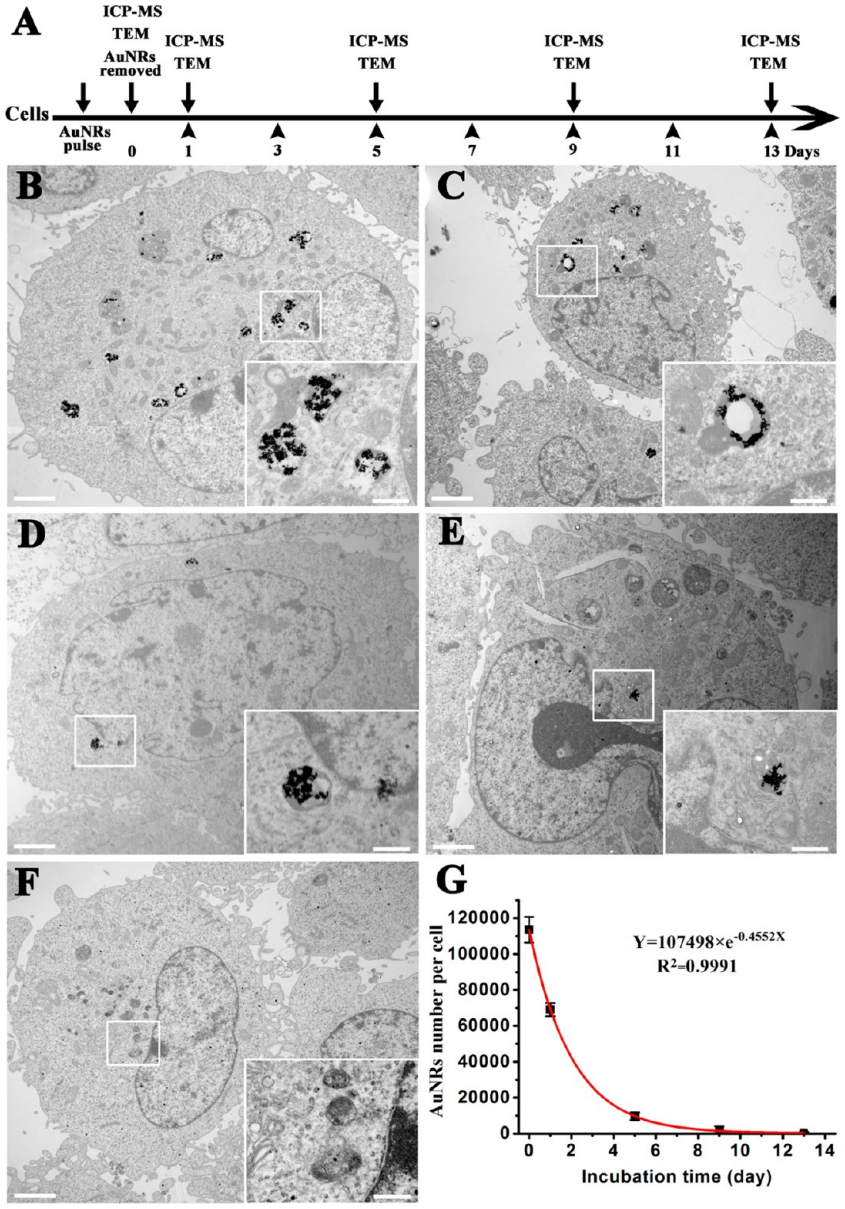

Figure 6. Dilution of intracellular AuNRs via cell proliferation. (A) Cells were pulsed with 60 pM AuNRs for 24 h and then were passaged every other day. The arrow heads represent the cell passaging. (B–F) Representative TEM images show the location of AuNRs in the cells after 0, 1, 5, 9, and 13 days of culture. The rectangle areas are further magnified at the bottom. The scale bars in the images and inserted images represent 2 and 0.5 μm, respectively. (G) The intracellular AuNRs number calculated according to the data measured by ICP-MS. The amount of AuNRs is expressed as AuNRs number in each cell.

exocytosis. Chemical inhibitors are commonly used to study endocytosis or exocytosis induced by nanoparticles.[40,41] Usually it takes several hours to conduct inhibitory treatment (for example concanamycin), while the exocytosis of AuNRs in our case was very fast, which was detected by TEM after 30 min incubation (Figure 2L). Hence it is not suitable to use inhibitory manner to track AuNRs exocytosis. Additionally, exocytosis inhibitors may not be able to block the exocytosis completely. To overcome these limitations, we conducted two experiments: (1) AuNR-chasing experiments: the cells were pulsed with AuNRs for 30 min, and then the location of AuNRs was chased in AuNR-free medium for 0.25–6 h using TEM. (2) Gold content in the supernatant was quantified by ICP-MS to characterize AuNRs exocytosis.

After 15 min of chasing, AuNRs associated with electron-dense materials ("dirty" AuNRs) were observed in lysosomes (Figure 5A). The dirty AuNRs at the membrane are exocytosed AuNRs (Figure 5B, C) rather than the uninternalized AuNRs because of the particular defects in endocytosis. Reasons are as follows: cells and extracellular components are composed of proteins, lipids, nucleic acids, etc., all of which have low electron density compared with gold nanorods. But undigested substances in lysosomes possess a high electron density. When the lysosomal contents are exocytosed, electron dense substances will be ejected out together with AuNRs and this accounted for AuNRs appearing near the cell surface adsorbed electron-dense substances.[16] Additionally, the number of dirty AuNRs near the cell membrane increased (Figure 5B, D, F, H, J) with the chasing time elongated, indicating AuNRs were

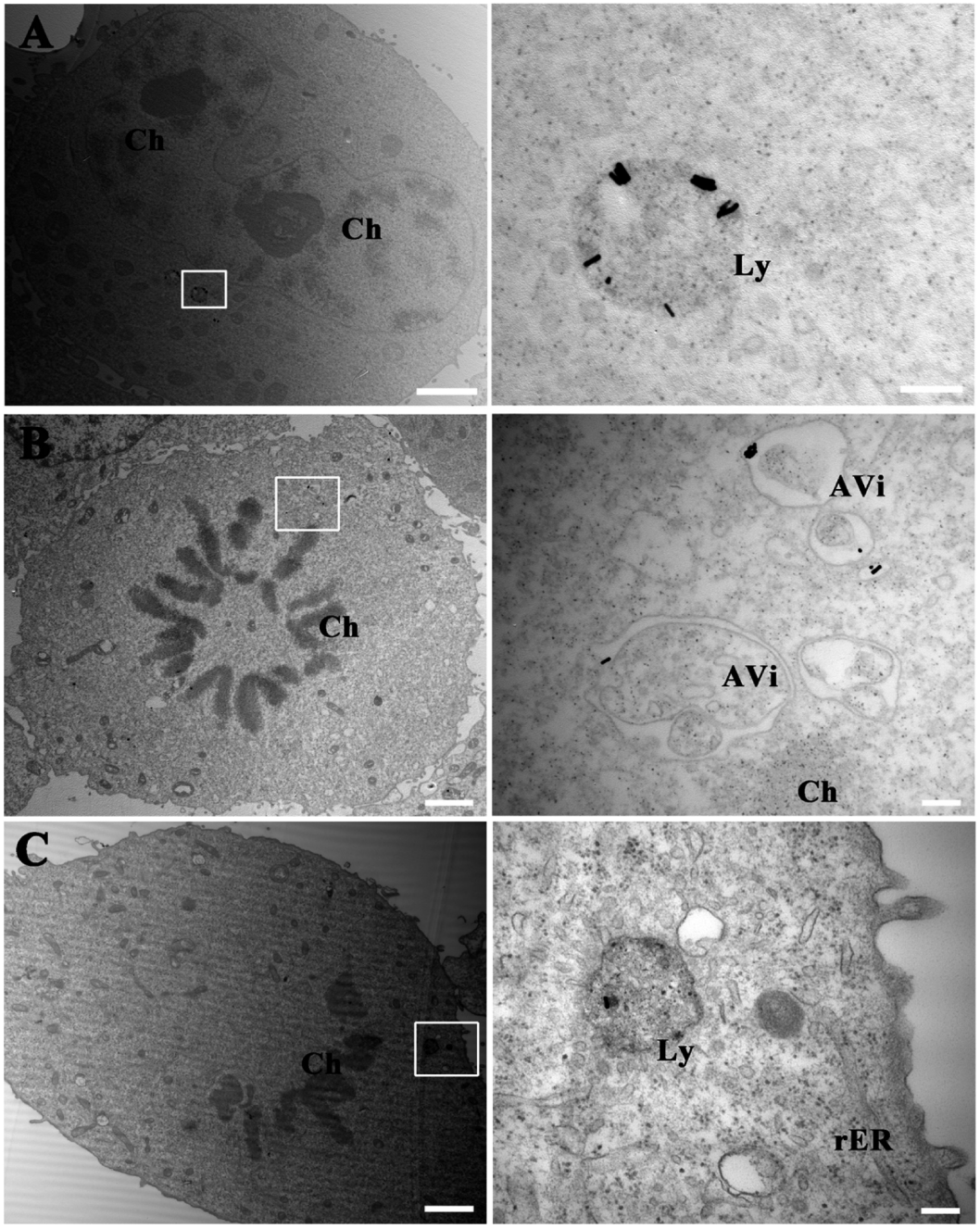

Figure 7. AuNRs are restrained in vesicular structures of the cells during mitosis. (A) prophase, (B) metaphase, (C) anaphase. The rectangular areas are further magnified at the right. The scale bars on the left and right column represent 2 μm and 200 nm, respectively. Ch, chromosome; Ly, lysosome; AVi, immature autophagosome; rER, rough endoplasmic reticulum.

successively expelled out (Figure 5D–J). After 6 h of chasing, AuNRs were also observed in RB (Figure 5K), and AuNRs in RB still can be expelled from cells similar to that in endosomes and lysosomes.[23] The ICP-MS results showed that gold content in the supernatants were significantly elevated from 15 to 30 min of chasing, confirming the exocytosis of AuNRs. It was striking to see that gold content in the supernatant then dropped to a plateau stage at 1, 2, and 6 h of chasing time points (Figure 5L), which strongly suggested the exocytosed AuNRs were re-endocytosed by the cells, otherwise gold in the supernatant would increase with chasing time elongated.

AuNRs Are Diluted by Cell Division. AuNRs dilution over time was clearly seen in our experiments (see the Supporting Information, Figure S3). To figure out AuNRs dilution behavior during cell proliferation, we continuously passaged AuNR-incubated cells for up to 13 days (about 13 times of cell doubling time) and examined with TEM observation together with ICP-MS analysis. The procedure is schematically illustrated in Figure 6A. With culture time increased, the number of AuNRs in the cells was reduced and no AuNRs were observed after 13 days (Figure 6B–F). Results from ICP-MS analysis demonstrated that the intracellular AuNRs number decreased exponentially (Figure 6G), which was inversely correlated to the trend of cell proliferation. The phenomenon suggested it was the cell division instead of

dx.doi.org/10.1021/am4033857 | ACS Appl. Mater. Interfaces 2013, 5, 9856–9865

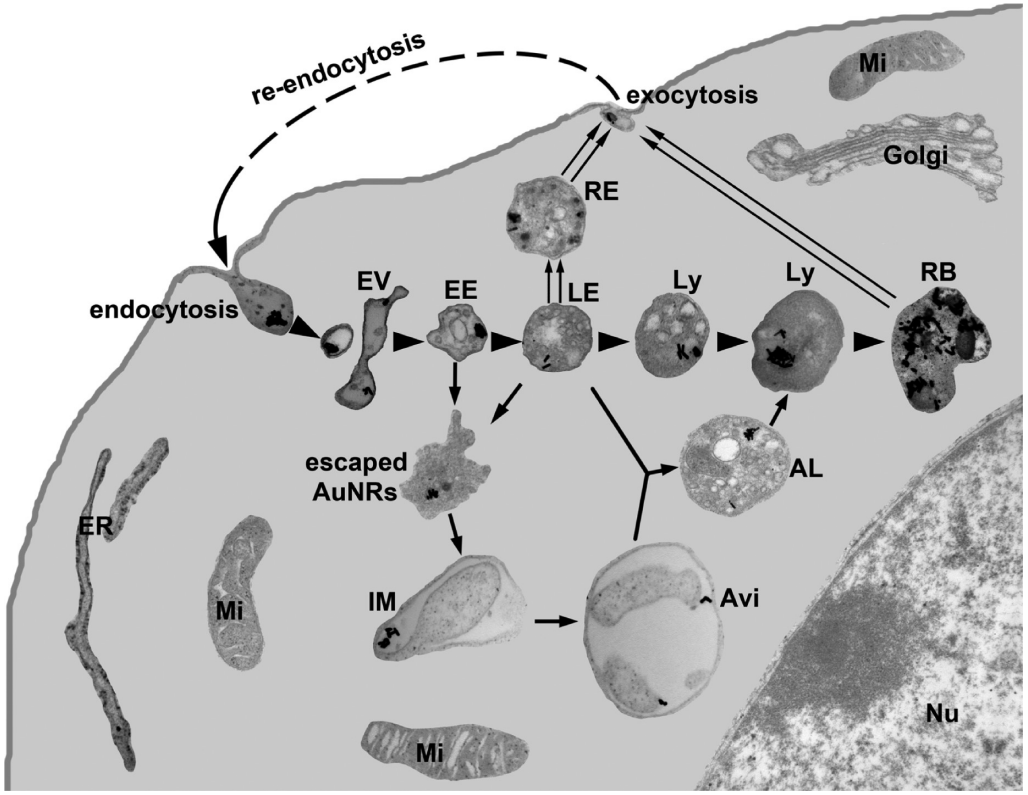

Figure 8. Schematic illustration of the trafficking of AuNRs in MDA-MB-231 cells. Arrow heads indicate AuNRs enter the lysosome maturation. Arrows point that escaped AuNRs are recycled back into lysosomes through autophagy. Double arrows demonstrate AuNRs in the lysosomal system are exocytosed. Dash arrow labels exocytosed AuNRs are re-endocytosed. EV, endocytic vesicle; EE, early endosome; LE, late endosome; Ly, lysosome; RB, residual body; RE, recycling endosome; Mi, mitochondria; Nu, nucleus; Golgi, golgi apparatus; ER, endoplasmic reticulum; IM, isolation membrane; AVi, immature autophagosome; AL, autolysosome.

exocytosis that diluted intracellular AuNRs as the exocytosed AuNRs could be re-endocytosed.

During the whole experimental process, most of the AuNRs were restricted in residual bodies in aggregated status and the rest were located in lysosomes and endosomes (Figure 6). Even though the cells were in prophase, metaphase, and anaphase, and nuclear membrane was dissolved in mitosis, AuNRs were still restrained in the vesicular structures (Figure 7). As shown by the Supporting Information, Movie S1, the cells could complete mitosis even with AuNRs inside. And most importantly, the movement of AuNRs aggregates (black dots in cells) was in coincidence with that of lysosomes in the cells, reaffirming that the AuNRs were sequestered in lysosomes. Because the partitioning of lysosomes in mitosis is highly ordered but imprecise,[42] the mitosis would lead to uneven distribution of AuNRs in daughter cells. This point was evidenced by TEM observation on the day 9 as most of the cells were AuNR-free, whereas the rest of cells contained AuNRs (see the Supporting Information, Figure S4). During the whole process, no AuNRs were observed in the nucleus, mitochondria, endoplasmic reticulum and Golgi apparatus of the cells. The restrictive location of AuNRs in the lysosomal system protected other important organelles from the direct contact with AuNRs.

CONCLUSIONS

AuNRs can be taken up quickly by the cells through endocytosis, and then enter lysosome maturation and end in residual body. Although AuNRs are expelled by cell exocytosis, they can be re-endocytosed by the cells. Very few of AuNRs were escaped from the vesicular system, but they could be recycled back into lysosomes by cytoprotective autophagy (Figure 8). The above processes affirm that the engulfed AuNRs are strictly confined to lysosomes and remain inside through mitosis. Generally, the trafficking of AuNRs in the cells partly explains the low cytotoxicity of them and provides detailed information for designing effective AuNR-based imaging contrast as well as drug delivery system. For example, future works of drug delivery can focus on enhancing the cytoplasmic delivery of AuNRs by inhibiting the autophagy process to increase the retention of escaped AuNRs in cytoplasm.

ASSOCIATED CONTENT

Supporting Information

Additional information as noted in the text. This material is available free of charge via the Internet at http://pubs.acs.org.

AUTHOR INFORMATION

Corresponding Authors

*E-mail: xuhy@pumc.edu.cn.
*E-mail: wuxc@nanoctr.cn.

Notes

The authors declare no competing financial interest.

ACKNOWLEDGMENTS

The authors thank the National Key Program of China (973 program 2010CB934002, 2011CB933504, 2011CB932802),

and Natural Science Foundation of China (NSFC 81000665) for financial support. The authors also thank Mr. Wei Dai from Core Instrument Faculty of IBMS (CAMS & PUMC) for his precious help in TEM sample preparation and ultrastructural observation.

REFERENCES

(1) Cobley, C. M.; Chen, J.; Cho, E. C.; Wang, L. V.; Xia, Y. *Chem. Soc. Rev.* **2011**, *40*, 44−56.
(2) Alkilany, A. M.; Thompson, L. B.; Boulos, S. P.; Sisco, P. N.; Murphy, C. J. *Adv. Drug Delivery Rev.* **2012**, *64*, 190−199.
(3) Oyelere, A. K.; Chen, P. C.; Huang, X.; El-Sayed, I. H.; El-Sayed, M. A. *Bioconjugate Chem.* **2007**, *18*, 1490−1497.
(4) Chen, J.; Irudayaraj, J. *ACS Nano* **2009**, *3*, 4071−4079.
(5) Chithrani, B. D.; Chan, W. C. *Nano Lett.* **2007**, *7*, 1542−1550.
(6) Zhang, W.; Meng, J.; Ji, Y.; Li, X.; Kong, H.; Wu, X.; Xu, H. *Nanoscale* **2011**, *3*, 3923−3932.
(7) Pangarkar, C.; Dinh, A. T.; Mitragotri, S. *J. Controlled Release* **2012**, *162*, 76−83.
(8) Dominska, M.; Dykxhoorn, D. M. *J. Cell Sci.* **2010**, *123*, 1183−1189.
(9) Taylor, A.; Wilson, K. M.; Murray, P.; Fernig, D. G.; Lévy, R. *Chem. Soc. Rev.* **2012**, *41*, 2707−2717.
(10) Alkilany, A. M.; Nagaria, P. K.; Hexel, C. R.; Shaw, T. J.; Murphy, C. J.; Wyatt, M. D. *Small* **2009**, *5*, 701−708.
(11) Parab, J. H.; Chen, H. M.; Lai, T.; Huang, J. H.; Chen, P. H.; Liu, R. S.; Hsiao, M.; Chen, C. H.; Tsai, D. P.; Hwu, Y. K. *J. Phys. Chem. C* **2009**, *113*, 7574−7578.
(12) Qiu, Y.; Liu, Y.; Wang, L.; Xu, L.; Bai, R.; Ji, Y.; Wu, X.; Zhao, Y.; Li, Y.; Chen, C. *Biomaterials* **2010**, *31*, 7606−7619.
(13) Rosman, C.; Pierrat, S.; Henkel, A.; Tarantola, M.; Schneider, D.; Sunnick, E.; Janshoff, A.; Sönnichsen, C. *Small* **2012**, *8*, 3683−3690.
(14) Li, J. L.; Gu, M. *Biomaterials* **2010**, *31*, 9492−9498.
(15) Jang, B.; Choi, Y. *Theranostics* **2012**, *2*, 190−197.
(16) Harding, C.; Heuser, J.; Stahl, P. *J. Cell Biol.* **1983**, *97*, 329−339.
(17) Kleijmeer, M. J.; Morkowski, S.; Griffith, J. M.; Rudensky, A. Y.; Geuze, H. J. *J. Cell Biol.* **1997**, *139*, 639−649.
(18) Huotari, J.; Helenius, A. *EMBO J.* **2011**, *30*, 3481−3500.
(19) Chang, J. P.; Gibley, C. W., Jr. *Cancer Res.* **1968**, *28*, 521−534.
(20) Feng, L.; Wu, X.; Ren, L.; Xiang, Y.; He, W.; Zhang, K.; Zhou, W.; Xie, S. *Chem.—Eur. J.* **2008**, *14*, 9764−9771.
(21) Firat-Karalar, E. N.; Welch, M. D. *Curr. Opin. Cell Biol.* **2011**, *23*, 4−13.
(22) Sakai, J.; Li, J.; Subramanian, K. K.; Mondal, S.; Bajrami, B.; Hattori, H.; Jia, Y.; Dickinson, B. C.; Zhong, J.; Ye, K.; Chang, C. J.; Ho, Y. S.; Zhou, J.; Luo, H. R. *Immunity* **2012**, *37*, 1037−1049.
(23) Krishna, V. S. In *Comprehensive Biotechnology II: Including Cell Biology, Genetics Microbiology and Immunology*, 1st ed.; New Age International: New Delhi, India, 2006; p 42−91.
(24) Conner, S. D.; Schmid, S. L. *Nature* **2003**, *422*, 37−44.
(25) Canton, I.; Battaglia, G. *Chem. Soc. Rev.* **2012**, *41*, 2718−2739.
(26) Wang, L.; Liu, Y.; Li, W.; Jiang, X.; Ji, Y.; Wu, X.; Xu, L.; Qiu, Y.; Zhao, K.; Wei, T.; Li, Y.; Zhao, Y.; Chen, C. *Nano Lett.* **2011**, *11*, 772−780.
(27) Luzio, J. P.; Pryor, P. R.; Bright, N. A. *Nat. Rev. Mol. Cell Biol.* **2007**, *8*, 622−632.
(28) Zhang, W.; Ji, Y.; Meng, J.; Wu, X.; Xu, H. *PLoS ONE* **2012**, *7*, e31957.
(29) Shi, X.; von dem Bussche, A.; Hurt, R. H.; Kane, A. B.; Gao, H. *Nat. Nanotechnol.* **2011**, *6*, 714−719.
(30) Li, Y.; Yue, T.; Yang, K.; Zhang, X. *Biomaterials* **2012**, *33*, 4965−4973.
(31) Longatti, A.; Tooze, S. A. *Cell Death Differ.* **2009**, *16*, 956−965.
(32) Fairn, G. D.; Grinstein, S. *Trends Immunol.* **2012**, *33*, 397−405.
(33) Nakagawa, I.; Amano, A.; Mizushima, N.; Yamamoto, A.; Yamaguchi, H.; Kamimoto, T.; Nara, A.; Funao, J.; Nakata, M.; Tsuda, K.; Hamada, S.; Yoshimori, T. *Science* **2004**, *306*, 1037−1040.
(34) Kimura, S.; Fujita, N.; Noda, T.; Yoshimori, T. *Methods Enzymol.* **2009**, *452*, 1−12.
(35) Mizushima, N.; Yoshimori, T.; Levine, B. *Cell* **2010**, *140*, 313−326.
(36) Ma, X.; Wu, Y.; Jin, S.; Tian, Y.; Zhang, X.; Zhao, Y.; Yu, L.; Liang, X. J. *ACS Nano* **2011**, *5*, 8629−8639.
(37) Stern, S. T.; Adiseshaiah, P. P.; Crist, R. M. *Part. Fibre Toxicol.* **2012**, *9*, 20.
(38) Zhao, Y.; Howe, J. L.; Yu, Z.; Leong, D. T.; Chu, J. J.; Loo, J. S.; Ng, K. W. *Small* **2013**, *9*, 387−392.
(39) Hussain, S.; Al-Nsour, F.; Rice, A. B.; Marshburn, J.; Yingling, B.; Ji, Z.; Zink, J. I.; Walker, N. J.; Garantziotis, S. *ACS Nano* **2012**, *6*, 5820−5829.
(40) Setyawati, M. I.; Tay, C. Y.; Chia, S. L.; Goh, S. L.; Fang, W.; Neo, M. J.; Chong, H. C.; Tan, S. M.; Loo, S. C.; Ng, K. W.; Xie, J. P.; Ong, C. N.; Tan, N. S.; Leong, D. T. *Nat. Commun.* **2013**, *4*, 1673.
(41) Youssef, G.; Gerner, L.; Naeem, A. S.; Ralph, O.; Ono, M.; O'Neill, C. A.; O'Shaughnessy, R. F. *Dev. Biol.* **2013**, *380*, 274−285.
(42) Bergeland, T.; Widerberg, J.; Bakke, O.; Nordeng, T. W. *Curr. Biol.* **2001**, *11*, 644−651.